

Highlights

Energy Management System for Resilience-Oriented Operation of Ship Power Systems

Thai-Thanh Nguyen, Bang Le-Huy Nguyen, Tuyen Vu

- A resilience-oriented energy management system of ship power systems is proposed.
- Multiple types of energy storage systems such as battery energy storage and supercapacitor energy storage systems are considered.
- Multi-objective optimization problem and gradient descent algorithm are proposed to balance the trade-off between multiple objectives.
- A comparison study between the receding horizon optimization and fixed horizon optimization is presented.
- Proposed receding horizon optimization for ship power systems enables real-time implementations.

Energy Management System for Resilience-Oriented Operation of Ship Power Systems

Thai-Thanh Nguyen^a, Bang Le-Huy Nguyen^a and Tuyen Vu^{a,*}

^aClarkson University, Potsdam, NY, USA

ARTICLE INFO

Keywords:

Energy management
Ship power system
Resilience
Load shedding
Energy storage system
Receding horizon optimization.

ABSTRACT

This paper proposes an original energy management methodology for enhancing the resilience of ship power systems considering multiple types of energy storage systems, including battery energy storage systems (BESS) and supercapacitor energy storage systems (SCES). The primary function of the proposed EMS is to maximize the load operability while taking ramp-rate characteristics of energy storage systems (ESS) and generators into account innovatively. Balancing BESS's state-of-charge (SoC) and prioritizing the SoC level of SCES are two additional objectives of the proposed EMS to manage energy storage systems. The receding horizon optimization (RHO) technique is proposed to reduce the computational burden, making the proposed method feasible for real-time applications. An all-electric MVDC ship power system is used to evaluate the performance of the proposed methodology. Simulation studies and results demonstrate the effectiveness of the proposed method in managing the ESS to ensure the system's resilience under generation power shortage. In addition, the proposed RHO technique significantly reduces the computation burden seen in the FHO technique while maintaining an acceptable resilience performance.

1. Introduction

Modern shipboard power systems (SPS) are shifting toward all-electric ships (AES), which integrate advanced systems such as electric propulsion, power conversion, energy storage systems (ESS), and intelligent management systems. Electrifying SPS enables the uses of ESS for improving fuel efficiency [1–3] and serving high power ramp-rate loads [4]. Due to the vulnerability of SPS to system failures such as tripping generations, ESS devices can be utilized as backup sources to compensate for power shortages caused by tripping generation units [5, 6].

ESS integrated into ships can be categorized into two types based on their characteristics. The first has high energy density but low power density, while the second has high power density but low energy density [7]. Battery energy storage systems (BESS) belong to the first type, which can operate for a relatively long period of time. The second type includes super-capacitor energy storage systems (SCES), which can generate high power for a short period of time. The uses of both types will offer benefits of high power density and high energy density. BESS can be used to serve base loads and moderate ramp-rate loads whereas SCES serve critical high ramp-rate loads [8, 9]. The uses of hybrid ESS, including BESS and SCES in AES, have been presented in [10–12], in which fuzzy controls were used to manage hybrid ESS system for SPS with pulsed loads. Either low-pass filter [10] or high-pass filter [11] could be used to separate the low and high-frequency components, then the fuzzy controls are used to produce the reference signals for the BESS and SCES accordingly. Model predictive

controls of hybrid ESS for mitigating fluctuation in loads and increasing fuel efficiency have been presented in [13, 14]. Optimal power flow for ship power systems with hybrid ESS was presented in [15]. Although these strategies deal with energy management of hybrid ESS, they might fail to manage SPS in conditions of generation shortages, such as tripping generators. In such conditions, load shedding control is required to maintain power balance. Effectively managing hybrid ESS will minimize load shedding amount and enhance system resilience over a full mission scenario. A resilience-oriented energy management system (EMS) considering different characteristics of ESS plays an important role in future SPS.

The objective of the resilience-oriented operation of ship power systems is to minimize the amount of load shedding due to the failures of generations or operation of high power ramp-rate load (HRRL). The importance of loads can be categorized into vital or non-vital loads, which are defined by the weight values. When the available power generation is less than load demands, the non-vital loads (those with the low weight values) should be shed first. Existing studies on the resilience enhancement of SPS can be divided into two categories: centralized and decentralized approaches. In the centralized approach, the optimization problem is solved by a single control center, whereas in the decentralized approach, it is solved by multiple control units.

Centralized EMS for enhancing the resilience of ship power systems based on probabilistic methods have been presented in [16–19]. Dynamic prioritization of the loads was considered for load shedding problem in [20, 21]. However, ESS were excluded from these studies. Optimal power management in [22] performs load shedding and reconfiguration to minimize the impact of fault on ship power systems. A two-phase optimization problem to improve resilience was proposed in [23], in which the first phase of the optimization

This material is based upon research supported by, or in part by, the U.S. Office of Naval Research under award number N00014-16-1-2956

*Corresponding author

✉ tnguyen@clarkson.edu (T. Nguyen); nguyennb1@clarkson.edu (B.L. Nguyen); tvu@clarkson.edu (T. Vu)

Nomenclature

Abbreviations

AES	All-electric ship
BESS	Battery energy storage system
EMS	Energy management system
ESM	Energy storage module
ESS	Energy storage system
FHO	Fixed horizon optimization
HRRL	High ramp rate load
IPNC	Integrated power node center
PCM-1A	Power conversion module
PGM	Power generation module
PMM	Propulsion motor module
RHO	Receding horizon optimization
SCESS	Super-capacitor energy storage system
SoC	State-of-charge
SPS	Ship power system

Constants

α_e	Weight of SoC
n_E	Number of ESSs

n_G	Number of generators
n_L	Number of loads
N_p	Optimization horizon length
T	Mission time
w_i	Load weight

Indices and sets

e	ESS index
g	Generator index
i	Load index
t	Time index

Variables

o_i^t	Operation status of load
$P_e^{E,t}$	ESS power
$P_g^{G,t}$	Generator power
$r_e^{E,t}$	Power ramp rate of ESS
$r_g^{G,t}$	Power ramp rate of generator
u_p^t	Auxiliary variable of absolute ESS power
u_{SoC}^t	Auxiliary variable of SoC difference

problem maximizes load survivability, whereas the second phase maximizes the functionality of supplying loads. A graph-theoretic method considering line capacities and load priorities was used in [24] to enhance system resilience against physical attacks on power lines. Although ESS are also not involved in [22–24], the optimization problems in these studies are still complex and challenging to solve. Thus, constraint relaxation was utilized to formulate a new low-complexity problem that ensures feasible near-optimal solutions. With the inclusion of several types of ESS, the complexity of existing centralized optimization problems will increase significantly, which poses a considerable impact on the computational burden.

Distributed strategies in [25–30] overcome the computational limitation of the centralized approaches as the global optimization problem is solved by multiple controllers. In [25–28], the ship power system was divided into multiple zones and the distributed EMS based on the alternating direction method of multipliers algorithm were used to solve the optimization in the distributed manner. In [29, 30], multi-agent approaches were presented to manage load shedding in ship power systems. However, limitations of these distributed EMS are the complexity of communication systems and the cyber-security issues due to their dependency on communication networks. The decentralized method in [31] manages hybrid ESS based on local voltage profiles, avoiding the use of complex communication networks. However, decentralized EMS in [31] neglects load shedding problem might put the ship power system at risk due to the potential insufficient generation capacity.

Existing energy management approaches have their own advantages and disadvantages. The centralized methods have advantages of simplicity and high accuracy, but they have the drawback of being computationally intensive, especially when dealing with large numbers of variables [31]. The decentralized methods overcome the computational limitation of the centralized method as the problem is solved in a distributed manner, but they face cyber-security issues due to complex communication networks [32–34]. Existing studies on the resilience enhancement of ship power systems are either computationally intensive or facing cyber-security issues. To address the problem, this paper proposes a receding horizon optimization (RHO) for the resilience-oriented operation of the ship power systems. The proposed methodology has a computational benefit over existing centralized methods since the RHO solves the optimization problem with a sequence of short trajectories rather than a single large trajectory. The proposed method is comparable to the distributed methods in terms of computational effort, but it is simpler and easier to implement due to the absence of complex communication networks, thus reducing the risk of cyber attacks. In addition, existing studies have not considered the energy management of multiple ESS, such as balancing SoC among ESS or prioritizing the use of ESS, in addition to the main objective of resilience enhancement. Since the SoC estimation is not perfect, the long time operation would cause large SoC variances among ESS. Prioritizing specific type of ESS for a particular role is an important factor as different types of ESS have different characteristics. SoC balancing and ESS prioritizing are

two secondary objectives being considered in the proposed EMS. The proposed methodology is evaluated in the four-zone notional MVDC system. A comparison study on the proposed RHO and FHO methods is also carried out.

The main contributions of this paper are as follows:

- A resilience-oriented EMS is proposed for ship power systems that include multiple types of ESS, such as BESS and SCESS.
- The proposed EMS not only enhances the system resilience but also manages ESS for long-term operation, such as balancing SoC among ESS and prioritizing the SoC level of SCESS.
- Receding horizon optimization is proposed to solve the optimization problem, which significantly reduces the computational burden, making it suitable for the real-time application.

The rest of this paper is organized as follows: Section 2 describes the resilience problem of ship power systems and formulating resilience enhancement into an optimization problem. The objective function and constraints are presented in this section. The proposed receding horizon optimization is presented in Section 3. Case studies of notional four-zone MVDC ship power systems are described in Section 4. A comparison study on the RHO and FHO methods is also given in this section. Finally, the main findings of this paper are summarized in Section 5.

2. Problem Formulation

The importance of loads is defined by a weight value w_i . For example, the vital load may have a weight of 1, and the non-vital load may have a weight of 0.1. The importance of loads can vary according to the mission operations, resulting in the variation of load's weight in different missions. Load operability (O) quantifies the degree of served loads, as given by (1), which is modified from [35] to ensure that the importance of loads and corresponding rated power are involved in load shedding problems. The resilience of ship power systems is enhanced by optimally scheduling generators and ESS to minimize load shedding, thus maximizing load operability.

$$O = \frac{\int_{t_0}^{t_f} \sum_{i=1}^{n_L} \hat{w}_i o_i^t dt}{\int_{t_0}^{t_f} \sum_{i=1}^{n_L} \hat{w}_i o_i^{*t} dt}, \quad (1)$$

$$\hat{w}_i = w_i P_{Li}^{rated} \quad \forall i \in n_L, \quad (2)$$

where n_L is the number of loads; P_{Li}^{rated} is the rated power of load i ; \hat{w}_i is the normalized weight value of load i ; o_i^t is the operational status of load i at time t ; and o_i^{*t} is the commanded operational status of load i ; t_0 represents the start time of the event, while t_f represents the end time of the event.

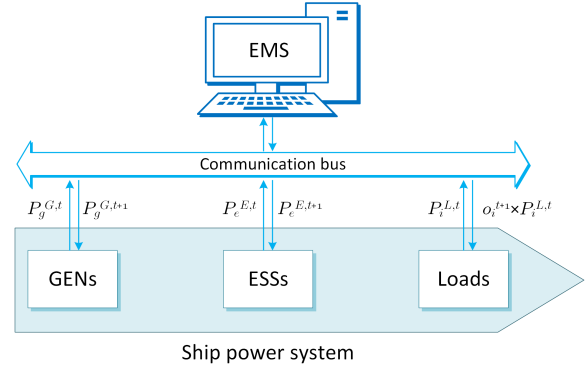


Figure 1: Energy management of ship power systems.

Fig. 1 shows the EMS of the ship power system, including communication signals. The centralized EMS gathers all information of the generators (GEN), ESS, and loads then the optimization process is performed to find the operational status of loads and power of GEN and ESS. Those optimal values are sent back to the ship power system as the reference values. Local controllers of generators and ESS take actions to track the reference signals. Loads will be shed if the value of operational status is smaller than commanded operational status.

2.1. Objective Function

The objective function for enhancing system resilience in the proposed EMS is given by (3), which includes four terms, as shown in (5) to (8). The first term, $f_1(o_i^t)$, represents for load operability over mission time T . The second term, $f_2(P_e^{E,t})$, is used to minimize control actions of ESS. The third term, $f_3(SoC^t)$, minimizes the state-of-charge (SoC) difference between ESS. The final term, $f_4(SoC^T)$, is used to maximize SoC at the end of the optimization window, which makes the proposed method distinguish from existing optimization algorithms that maintain the same SoC levels at initial and final intervals of the optimization window. The final term of objective function helps the receding horizon optimization maintaining SoC level for long-term operation.

$$\max_x \quad f(x) = f_1(o_i^t) - \omega_1 f_2(P_e^{E,t}) - \omega_2 f_3(SoC^t) + \omega_3 f_4(SoC^T), \quad (3)$$

$$x = [o_i^t, P_e^{E,t}, P_g^{G,t}]^T, \quad (4)$$

$$f_1(o_i^t) = \sum_{i=1}^T \sum_{i=1}^{n_L} \hat{w}_i o_i^t, \quad (5)$$

$$f_2(P_e^{E,t}) = \sum_{i=1}^T \sum_{e=1}^{n_E} |P_e^{E,t}|, \quad (6)$$

$$f_3(SoC^t) = \sum_{i=1}^T \sum_{l,m} |SoC_l^{E,t} - SoC_m^{E,t}|, \quad (7)$$

$$f_4(SoC^T) = \sum_{e \in 1}^{n_E} \alpha_e SoC_e^{E,T}, \quad (8)$$

where T is the mission time; o_i^t is the operability of load i at time t ; \hat{w}_i is the weight of load i , which indicates the importance of load such as critical or non critical loads; $P_e^{E,t}$ is the active power of ESS e at time t ; SoC^t is the ESS's SoC at time t ; and SoC^T is the ESS's SoC at the end of optimization window; ω_1, ω_2 , and ω_3 are the constant weights, which will be optimally selected by the gradient descent algorithm in the next section.

2.2. Constraints

Objective function (3) is subjected to power supply-demand constraint given in (9), as the optimal load operability has to be smaller than total generations including ESS power.

$$\sum_{i=1}^{n_L} P_i^{L,t} o_i^t \leq \sum_{e=1}^{n_E} P_e^{E,t} + \sum_{g=1}^{n_G} P_g^{G,t} \quad \forall t \in T, \quad (9)$$

where n_L is the number of loads; $P_i^{L,t}$ is the command of load i at time t ; n_E is the number of ESS; n_G is the number of generations; and P_g^G is the power of generator g .

Operational status o_i^t is subjected to the limit constraints (10), in which the commanded operational status is equal to one ($o_i^{*t} = 1$). If $o_i^t = 0$, load i must be shed 100% at time t ; if $o_i^t = 1$, load i is served 100% at time t . In addition, ESS and generators are also subjected to the limit constraints in (11) and (12).

$$0 \leq o_i^t \leq 1 \quad \forall i \in n_L, \forall t \in T, \quad (10)$$

$$P_e^{\min} \leq P_e^{E,t} \leq P_e^{\max} \quad \forall e \in n_E, \forall t \in T, \quad (11)$$

$$P_g^{\min} \leq P_g^{G,t} \leq P_g^{\max} \quad \forall g \in n_G, \forall t \in T, \quad (12)$$

where P_e^{\min} and P_e^{\max} are the minimum and maximum capacity of ESS, respectively; P_g^{\min} and P_g^{\max} are the minimum and maximum capacity of generator, respectively.

Since some loads have discrete changes, the operational status of such loads is subjected to the discrete function, as given by (13).

$$o_i^t \in \begin{cases} \mathcal{Z} & \text{if load } i \text{ is the step load,} \\ [0, 1] & \text{otherwise,} \end{cases} \quad (13)$$

where $\mathcal{Z} = \{0 : \Delta o_i : 1\}$; $\Delta o_i = 1/n$; $n \in \mathbb{Z}^+$ is the number of steps of the load command.

Since both generators and ESS have limit on power ramp-rate, reference power set points to these devices is subjected to ramp-rate constraints (14) and (15).

$$r_g^{\min} \leq r_g^{G,t} \leq r_g^{\max} \quad \forall g \in n_G, \forall t \in T, \quad (14)$$

$$r_e^{\min} \leq r_e^{E,t} \leq r_e^{\max} \quad \forall e \in n_E, \forall t \in T, \quad (15)$$

$$r_g^{G,t} = \frac{P_g^{G,t} - P_g^{G,t-1}}{\Delta t} \quad \forall g \in n_G, \forall t \in T, \quad (16)$$

$$r_e^{E,t} = \frac{P_e^{E,t} - P_e^{E,t-1}}{\Delta t} \quad \forall e \in n_E, \forall t \in T, \quad (17)$$

where Δt is the sampling time.

Finally, to prevent dip charge and discharge of ESS, the SoC level has to be in limit (18).

$$SoC_e^{\min} \leq SoC_e^{E,t} \leq SoC_e^{\max} \quad \forall e \in n_E, \forall t \in T, \quad (18)$$

$$SoC_e^{E,t} = SoC_e^{E,t-1} + \Delta t \frac{P_e^{E,t}}{P_e^{\max}} \quad \forall e \in n_E, \forall t \in T. \quad (19)$$

2.3. MILP to Solve Optimization Problem

The problem formulated from Section 2 includes discrete variable of operational status and non-linear objective terms (f_2 and f_3). To solve (3) by the mixed-integer linear programming (MILP), the discrete variable is converted to integer variable and the non-linear objective terms are linearized.

To convert discrete variable to integer variable, the load power ($P_i^{L,t}$) and load weight value (\hat{w}_i) of the discrete loads are scaled with the a factor of step size (Δo_i), as given in (20) and (21).

$$\hat{w}_i = \hat{w}_i \Delta o_i \quad (20)$$

$$\hat{P}_i^{L,t} = P_i^{L,t} \Delta o_i \quad (21)$$

where \hat{w}_i and $\hat{P}_i^{L,t}$ are the modified load weight and power, respectively. Substituting (20) and (21) into (5) and (9), respectively, variable of operational status is converter to the integer variable subjected to the following constraint.

$$0 \leq o_i^t \leq \frac{1}{\Delta o_i} \quad (22)$$

The optimal variables of operation status found by optimization process are converted back to discrete variables using (23), which will be used as the load commands for the discrete loads.

$$\delta_i^t = o_i^t \Delta o_i \quad (23)$$

Non-linear objective terms are linearized by introducing auxiliary variables and constraints for such variables, as given by (24) and (25).

$$u_P^t = |P_e^{E,t}|, \quad (24)$$

$$u_{SoC}^t = |SoC_l^{E,t} - SoC_m^{E,t}| \quad (25)$$

Objective function (3) can be represented by (26) subjected to new constraints of operational status, power balance, and additional constraints of auxiliary variables. Thus,

MILP can be used to solve the problem (26).

$$\begin{aligned}
 \max_x \quad & f(x) = f_1(o_i^t) - \omega_1 f_2(u_p^t) \\
 & - \omega_2 f_3(u_{SoC}^t) + \omega_3 f_4(SoC^T) \\
 \text{s.t.} \quad & 0 \leq o_i^t \leq \frac{1}{\Delta o_i} \quad \forall i \in n_L, \forall t \in T, \\
 & \sum_{i=1}^{n_L} \hat{P}_i^{L,t} o_i^t \leq \sum_{e=1}^{n_{E,t}} P_e^{E,t} + \sum_{g=1}^{n_G} P_g^{G,t} \quad \forall t \in T, \\
 & 0 \leq u_p^t \leq P_e^{\max} \quad \forall e \in n_E, \forall t \in T, \\
 & u_p^t \geq P_e^{E,t} \quad \forall e \in n_E, \forall t \in T, \\
 & u_p^t \leq -P_e^{E,t} \quad \forall e \in n_E, \forall t \in T, \\
 & 0 \leq u_{SoC}^t \leq SoC_e^{\max} \quad \forall e \in n_E, \forall t \in T, \\
 & u_{SoC}^t \geq SoC_l^{E,t} - SoC_m^{E,t} \quad \forall l, m \in n_E, \forall t \in T, \\
 & u_{SoC}^t \geq -SoC_l^{E,t} + SoC_m^{E,t} \quad \forall l, m \in n_E, \forall t \in T,
 \end{aligned} \tag{26}$$

where

$$x = [o_i^t, P_e^{E,t}, P_g^{G,t}, u_p^t, u_{SoC}^t]^T, \tag{27}$$

$$f_1(o_i^t) = \sum_{i \in 1}^T \sum_{i \in 1}^{n_L} \hat{w}_i o_i^t, \tag{28}$$

$$f_2(u_p^t) = \sum_{i \in 1}^T \sum_{e \in 1}^{n_E} u_p^t, \tag{29}$$

$$f_3(u_{SoC}^t) = \sum_{i \in 1}^T \sum_{l, m} u_{SoC}^t. \tag{30}$$

2.4. Gradient descent Algorithm to Optimize Objective Weights

Constant weights, $\omega = [\omega_1, \omega_2, \omega_3]$, in objective function (3) have an impact on load operability (5), which is shown in Fig. 2. The increases of ω_1 and ω_3 result in the reduction of load operability. Because a high value of ω_1 prevents ESS actions, which results in shedding more loads. Besides, a high value of ω_3 makes ESS charge frequently to maximize SoC level, which also results in shedding more loads. On the other hand, constant weight ω_2 has a slight impact on load operability as it tries to balance the SoC level among ESS.

From above observation, it can be seen that function \bar{f} in (31) is convex. Gradient descent (GD) algorithm in **Algorithm 1** is used to find constant weights ω_i . GD stop iterations when absolute error of function \bar{f} is smaller than a pre-defined value $\epsilon = 10^{-4}$. Optimal weights found by GD algorithm are $\omega = [0.0056; 0.0321; 0.0541]$.

$$\bar{f} = -\bar{f}_1 + \bar{f}_2 + \bar{f}_3 - \bar{f}_4 \tag{31}$$

where \bar{f}_i is the normalized function of f_i .

The tested system, which consists of three generators with a total capacity of 45 MW, two units of 10MW-BESS,

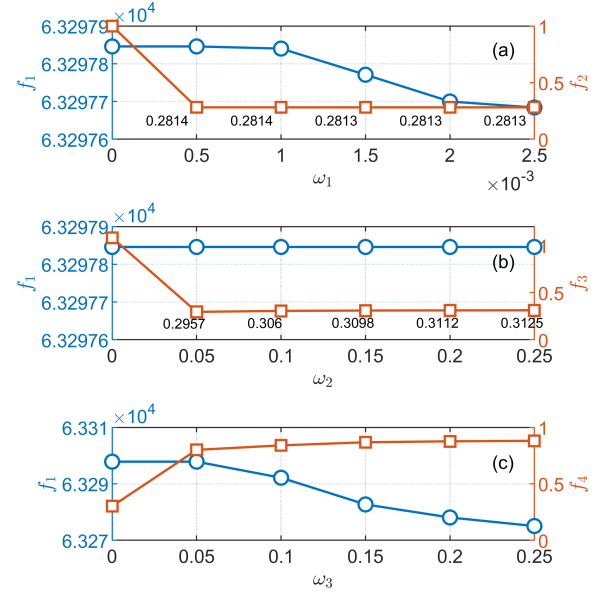


Figure 2: Effect of secondary objectives on load operability.

Algorithm 1 Optimizing weights based on GD algorithm.

- 1: $i \leftarrow 0$, initialize $\omega = [\omega_1; \omega_2; \omega_3]$
- 2: **repeat**
- 3: Calculate \bar{f} based on ω_1, ω_2 , and ω_3 : $\bar{f}(i) \leftarrow \bar{f}|\omega$;
- 4: $g(i) \leftarrow [\bar{f}(i) - \bar{f}(i-1)] / [\omega(i) - \omega(i-1)]$;
- 5: $\omega(i+1) \leftarrow \omega(i) - \gamma g(i)$;
- 6: $i \leftarrow i + 1$
- 7: **until** $|\bar{f}(i+1) - \bar{f}(i)| < \epsilon$
- 8: **return** ω ;

Table 1

System parameters

Symbol	Parameter	Value
n_E	Number of ESS	4
P_E^{\max}	ESS maximum power	10 MW
P_E^{\min}	ESS minimum power	-10 MW
$P_g^{\max, \min}$	Power ramp-rate limit of generator	± 1 MW/s
$r_{g, \max, \min}^{BESS}$	Power ramp-rate limit of BESS	± 5 MW/s
$r_{g, \max, \min}^{SCESS}$	Power ramp-rate limit of SCESS	± 100 MW/s
E_{BESS}	Energy level of BESS	1000 MJ
E_{SCESS}	Energy level of SCESS	200 MJ

and two units of 10MW-SCESS, are used to evaluate the effectiveness of the proposed GD algorithm on finding optimal weights. The energy of BESS and SCESS are given in Table 1. Maximum power generation is 85 MW. Fig. 3 shows the optimization results of the ship power system without considering secondary objective terms of f_1, f_2 , and f_3 . It can be seen in Fig. 3(a) that loads are mainly shed in the period from 80 s to 145 s. There are several issues, such as circulating power among ESS and low SoC levels of ESS at the end of optimization window, which might result in failure of ESS to serve loads in the next mission. In addition, the SoC levels are different among ESS.

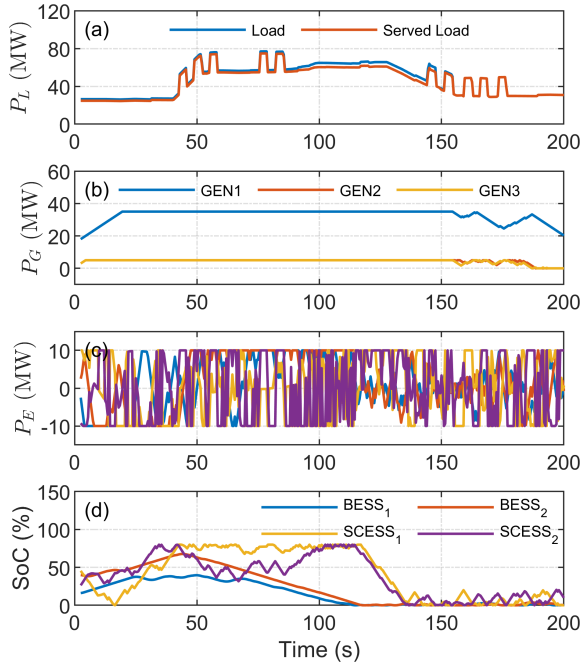


Figure 3: Optimization problem without secondary objectives (f_1 , f_2 , and f_3).

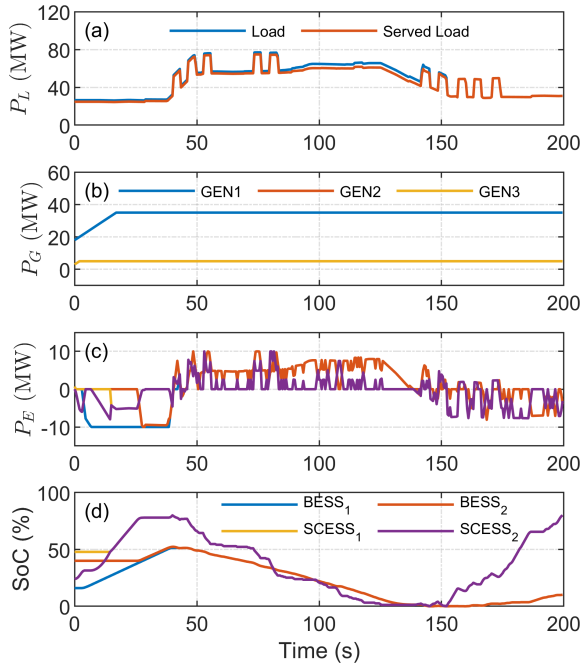


Figure 4: Optimization problem with optimal weights of secondary objectives.

Fig. 4 shows the optimization results considering secondary objectives with optimal constant weights. It can be seen that the above issues are addressed. Initial SoC levels of four ESS are different, however, they are equal after 30 s due to optimally scheduling ESS powers. SoC levels at the end of the optimization window are maximized to prepare for the next mission. In addition, since the SCESS are prioritized, their SoC levels are higher than those of BESS.

3. Proposed Receding Horizon Optimization

The optimization problem from (3) can be solved by the fixed horizon optimization (FHO) method, in which the optimization window is the whole mission time. Solving problem (3) yields the optimal operation status of the system in all time steps. However, the resilience operation of the ship power system requires a small control time step (0.5s) to fulfill the need of high ramp-rate loads. The required small time step causes the size of the optimization problem to increase significantly. The MILP problem creates additional challenge as they are highly nonlinear, which poses a significant impact on the computation required for real-time implementation.

To solve the above-mentioned problem, the receding horizon optimization (RHO) method is used in this paper. The RHO framework is designed with a series of shorter time windows to achieve the goal instead of one long trajectory as seen in the FHO method. The RHO-based optimization problem is solved at each time step to find a set of actions over a fixed time horizon (window), in which only first time-step solution of each window is applied to the physical system. The optimization process is repeated at the next time steps, in which a new optimization problem is solved when the time horizon shifted one step forward. The size of the MILP problem in RHO is substantially smaller than in FHO, making RHO suitable for real-time applications. The RHO method can involve real-time measurements at each time step as feedback to determine the optimal actions and even more accurate than FHO due to the system uncertainties. When the time horizon length is long enough to reach the goal, RHO is equivalent to the FHO method under the deterministic scenarios. The problem (26) is represented in the RHO problem, as in (32).

$$\max_x \quad f(x) = f_1(o_i^t) - \omega_1 f_2(u_p^t) - \omega_2 f_3(u_{SoC}^t) + \omega_3 f_4(SoC^T), \quad (32)$$

$$x = [o_i^t, P_e^{E,t}, P_g^{G,t}, u_p^t, u_{SoC}^t]^T, \quad (33)$$

$$f_1(o_i^t) = \sum_{i=1}^{N_p} \sum_{l=1}^{n_L} \hat{w}_l o_i^t, \quad (34)$$

$$f_2(P_e^{E,t}) = \sum_{i=1}^{N_p} \sum_{e=1}^{n_E} u_p^t, \quad (35)$$

$$f_3(SoC^t) = \sum_{i=1}^{N_p} \sum_{l,m} u_{SoC}^t, \quad (36)$$

$$f_4(SoC^T) = \sum_{e=1}^{n_E} \alpha_e SoC_e^{E,T}, \quad (37)$$

where N_p is the horizon length.

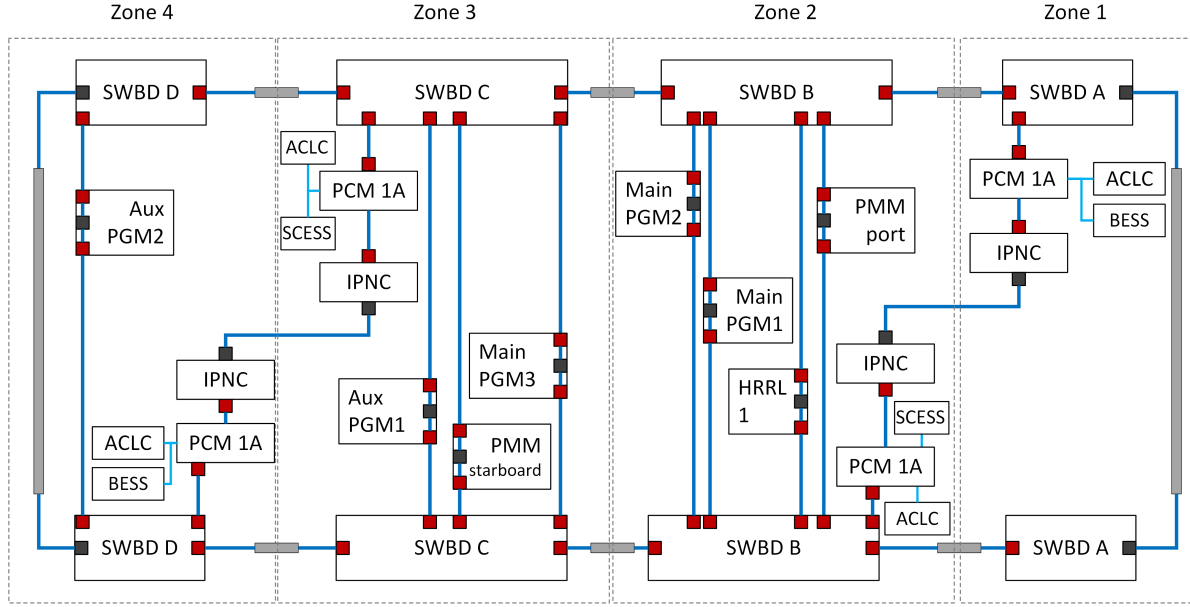


Figure 5: Notional four-zone MVDC shipboard power system adapted from [36].

 Table 2
RHO parameters

Symbol	Parameter	Value
Δt	Control sample time	0.5 s
N_p	Horizon length	60
T	Mission time	600 s

4. Case Studies

RHO is used to manage the ship power system under the condition of high ramp-rate load. A comparison with the FHO is presented in this section to show the effectiveness of the proposed RHO method.

4.1. System Description

The notional four-zone MVDC ship power system shown in Fig. 5 is used to evaluate the performance of the proposed EMS. The power rating of the shipboard power system is 100 MW. Each zone is composed of multiple modules such as power conversion module (PCM-1A), power generation module (PGM), propulsion motor module (PMM), integrated power node center (IPNC), and energy storage module (ESM). Parameters of the energy storage systems are given in Table 1 and the RHO parameters are given in Table 2. More detailed information on the MVDC shipboard power system can be found in [36].

4.2. Performance Evaluation

4.2.1. Performance under High ramp-rate Load Mission

The proposed RHO is evaluated in the condition of HRRL operation. In this condition, the ramp-rate of load power may exceed generation ramping. The uses of ESS,

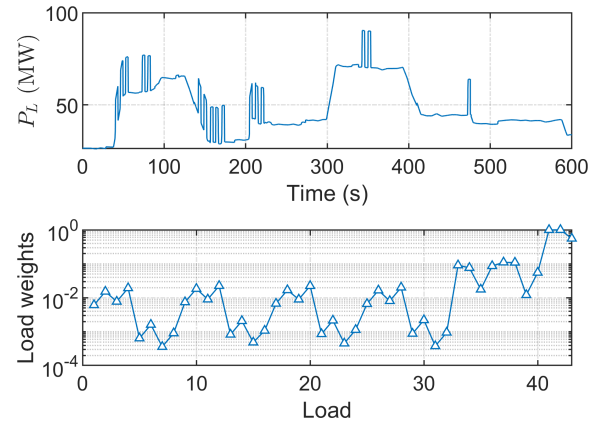


Figure 6: Load profile and weights of 43 loads.

particularly SCESS, can support the ship power system in this condition. The system 43 loads' profile and their weights are shown in Fig. 6.

The HRRL loads (load numbers 41, 42, and 43) have the largest weight values, which must be given top priority. Fig. 7(a) shows the load weights and optimal load operability that is found by two methods (RHO and FHO). When the load operability value is less than one, the load is shed. It can be seen that loads with low weight \hat{w}_i are shed while HRRL with the highest weight is served, which is depicted in Fig. 7(b). Fig. 8(a) shows the profiles of served load under two optimization methods. With the FHO method, more loads are shed before 300 s to serve for the increase in load demand from 300 s to 400 s, as depicted in Fig. 8(b). In the case of RHO, more loads are shed in period from 350 s to 400 s compared to FHO as RHO has shorter optimization length compared to FHO. The error of total load operability

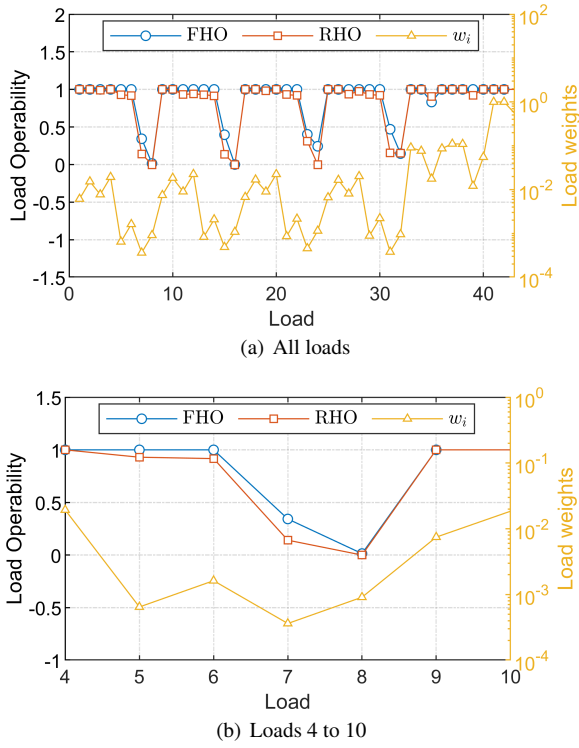


Figure 7: Compared load operability in HRRL mission.

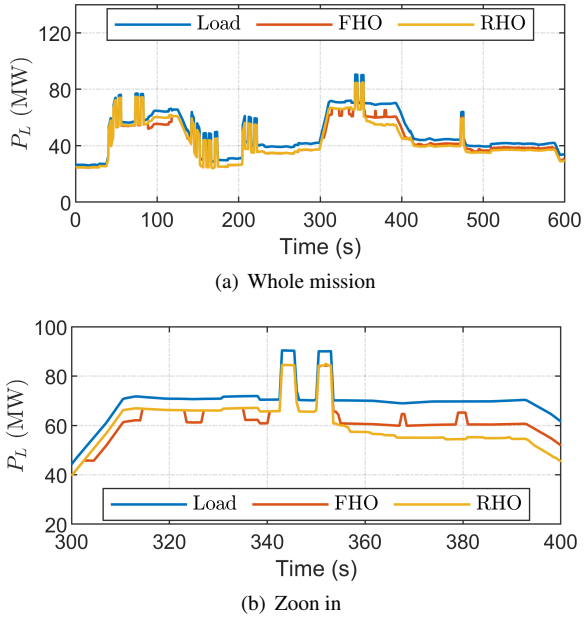


Figure 8: Load profile and served load under RHO and FHO methods.

between two methods given by (38) indicates that the performance of the proposed RHO is close to FHO.

$$\Delta f_1 = \frac{f_1^{FHO} - f_1^{RHO}}{f_1^{FHO}} = +0.05\% \quad (38)$$

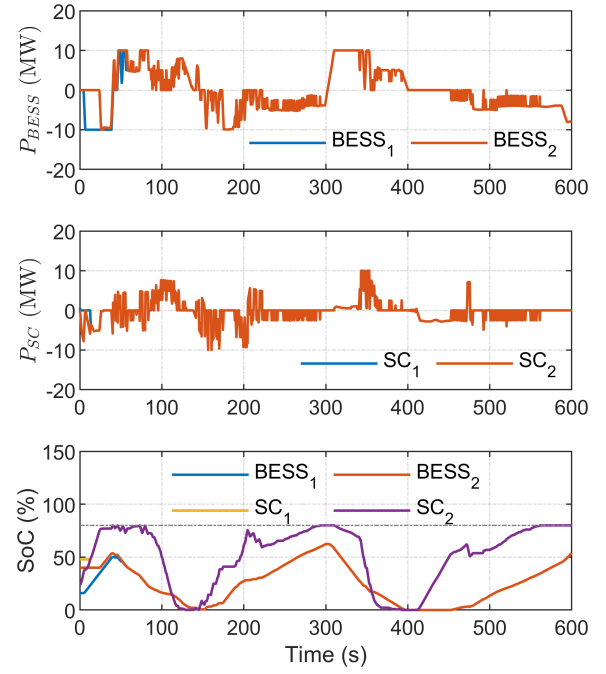


Figure 9: ESS power and energy when using RHO.

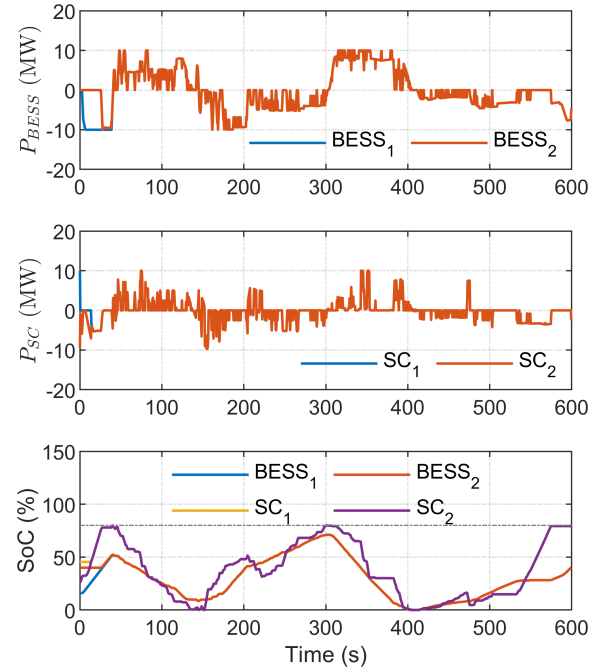


Figure 10: ESS power and energy when using FHO

The output power of BESS and SCESS are shown in Figs. 9 and 10. From 0 s to 50 s, four ESS are charged as the generation is larger than load demand. Since ESS have different SoC levels, the charging power of each ESS is different accordingly to balance SoC. It can be seen that two BESS and two SCESS have the same SoC levels after 50 s and the output power of either two BESS or two SCESS are the same. The maximum SoC level of ESS is kept at 80%. For both methods, SCESS are given priority to charge, resulting

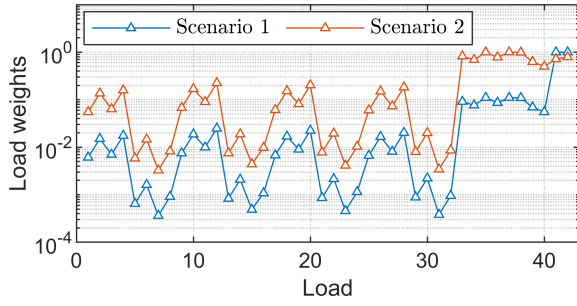


Figure 11: Weights of loads for different scenarios.

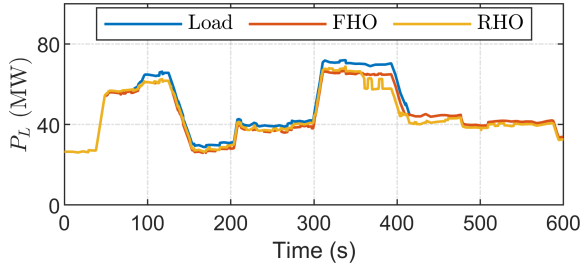


Figure 12: Served load in scenario 1.

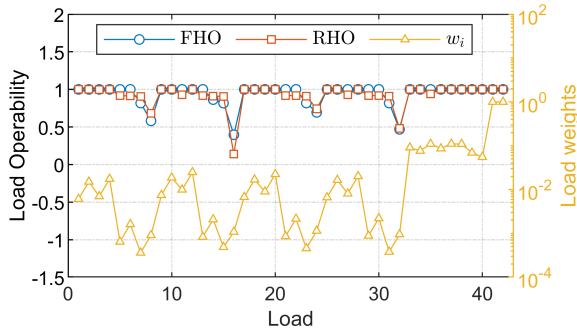


Figure 13: Compare load operability in scenario 1.

in higher SoC levels at the end of the optimization window compared to BESS. It is observed that the proposed RHO method achieves a similar performance yielded by the FHO method.

4.2.2. RHO Performance in Different Scenarios

The MVDC ship power system is operated under various scenarios such as peacetime cruise, sprint station, battle, and anchor [37]. The importance of loads varies with the operating conditions of the ship power system. A load might be vital in one scenario but not in another. For example, when the mission of the ship power system changes from cruise to battle, some loads that were previously non-vital become vital. The proposed RHO method is evaluated by two additional scenarios, as shown in Fig. 11.

Figs. 12 and 13 show the comparison between proposed RHO and FHO methods for the first scenario. Loads are mainly shed from 50 s to 400 s and only loads with low weight values are mainly shed, as shown in Fig. 13. Figs. 14 and 15 show the performance of RHO method compared

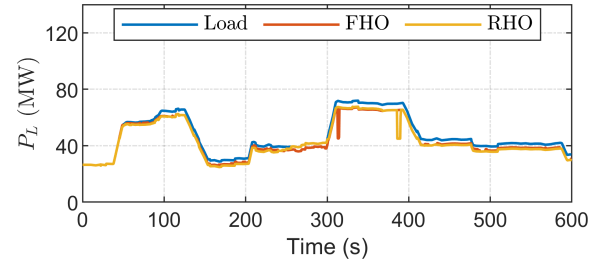


Figure 14: Served Load in scenario 2.

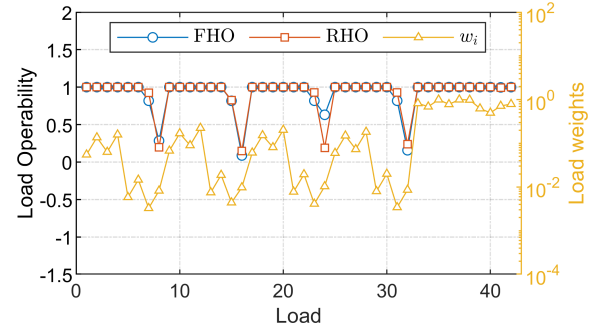


Figure 15: Compare load operability in scenario 2.

to FHO method for the second scenario. In this case, instead of shedding significant load at 314 s (FHO), RHO method sheds significant loads at 385 s. As the optimization window of RHO method is much shorter than that of FHO method, loads are still served at 314 s. However, all ESS are almost fully discharged after serving loads from 314 s to 384 s, loads are then shed significantly at 385 s due to the shortage of power generations. The total load operability shown in Figs. 13 and 15 indicates which loads are mainly shed in two scenarios. Non-vital loads with low weight values are primarily shed in both cases, whereas the vital loads with high weight values are served. Overall, it can be observed that the proposed RHO method achieves a similar performance compared to the FHO method.

4.3. Computational Comparison

The above sections presented two methods that achieve similar performance under various scenarios. A comparison between proposed RHO and FHO in Fig. 16 show the advantage of proposed RHO method in terms of computation. Both methods are performed on a processor of Intel@Core i7-10700H at 2.90 GHz and 64 GB RAM. The *intlinprog* function based on *primal-simplex* algorithm from MATLAB is used to solve the MILP problem. Various scenarios are conducted to evaluate the computational performance of both methods, such as HRRL, scenarios 1, and 2. In all scenarios, the total mission time is 600 s. In FHO method, the required RAM to solve the optimization problem is about 31~33 GB, whereas 1.6~1.7 GB RAM are required for RHO method. Despite using a powerful computer, FHO takes 1380~1440 s to solve the optimization problem. To ensure that the optimal solution can be found before applying the

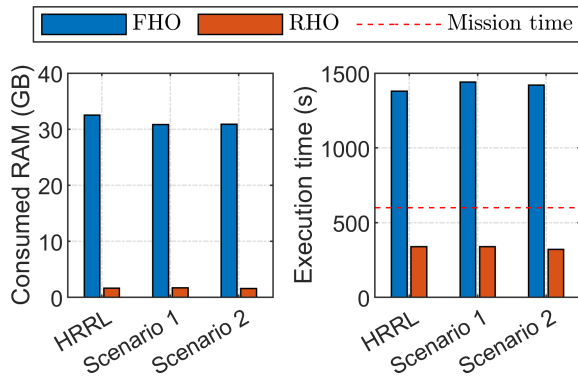


Figure 16: Computational comparison between RHO and FHO. Execution time in case of RHO method is the sum of execution time for all steps in 600s-mission.

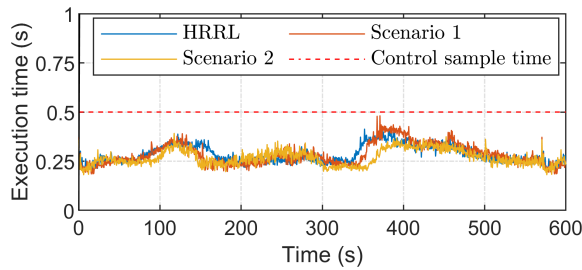


Figure 17: Execution time of the RHO method measured at each optimization step.

control actions, the execution time must be less than 600 s in the case of FHO, and in the case of RHO, the execution time at each step must be less than the control sample time of 0.5 s. It can be seen that the FHO method is not applicable for the real-time implementation of the required 600 s. In comparison, the proposed RHO method completes the optimization problem in less than 0.5 s, as shown in Fig. 17. Therefore, the RHO method is applicable for the real-time implementation. Compared to the FHO method, the proposed RHO method shows significant improvements in terms of computation as its RAM usage is 95% lower and its execution time is 76% faster.

5. Conclusion

A resilience-oriented EMS of ship power systems has been proposed in this paper, which manages multiple types of energy storage systems such as BESS and SCESS to maximize load operability. In addition to enhancing system resilience, secondary objectives of managing ESS were involved, such as balancing SoC among ESS and prioritizing the SoC level of SCESS. Since the power ramp-rate of SCESS is much higher than that of BESS, SCESS were given priority to serve HRRL. The gradient descent algorithm was proposed to optimally design the weights of secondary objectives. The RHO technique was proposed to reduce the computational burden, making it suitable for real-time applications. A comparison between RHO and FHO methods revealed that they produced comparable resilient results.

However, the use of the RHO method showed a significant improvement in computation, with significantly less RAM consumption and execution time. The paper assumed that the power cables have enough capacity to transfer power among subsystems. Our future research will consider the power line limits and deploy the proposed EMS in real-time controllers.

References

- [1] Hai Lan, Shuli Wen, Ying-Yi Hong, David C. Yu, and Lijun Zhang. Optimal sizing of hybrid pv/diesel/battery in ship power system. *Applied Energy*, 158:26–34, 2015. ISSN 0306-2619.
- [2] FD Kanellos. Optimal power management with ghg emissions limitation in all-electric ship power systems comprising energy storage systems. *IEEE Transactions on power systems*, 29(1):330–339, 2013.
- [3] Amjad Anvari-Moghaddam, Tomislav Dragicevic, Lexuan Meng, Bo Sun, and Josep M. Guerrero. Optimal planning and operation management of a ship electrical power system with energy storage system. In *IECON 2016 - 42nd Annual Conference of the IEEE Industrial Electronics Society*, pages 2095–2099, 2016. doi: 10.1109/IECON.2016.7793272.
- [4] Tuyen Van Vu, David Gonsoulin, Fernand Diaz, Chris S Edrington, and Touria El-Mezyani. Predictive control for energy management in ship power systems under high-power ramp rate loads. *IEEE Transactions on Energy Conversion*, 32(2):788–797, 2017.
- [5] R.D. Geertsma, R.R. Negenborn, K. Visser, and J.J. Hopman. Design and control of hybrid power and propulsion systems for smart ships: A review of developments. *Applied Energy*, 194:30–54, 2017. ISSN 0306-2619.
- [6] Shuli Wen, Hai Lan, Ying-Yi Hong, C Yu David, Lijun Zhang, and Peng Cheng. Allocation of ess by interval optimization method considering impact of ship swinging on hybrid pv/diesel ship power system. *Applied Energy*, 175:158–167, 2016.
- [7] Pengcheng Pan, Yuwei Sun, Chengqing Yuan, Xiping Yan, and Xujing Tang. Research progress on ship power systems integrated with new energy sources: A review. *Renewable and Sustainable Energy Reviews*, 144:111048, 2021. ISSN 1364-0321.
- [8] Sidun Fang, Yan Xu, Zhengmao Li, Tianyang Zhao, and Hongdong Wang. Two-step multi-objective management of hybrid energy storage system in all-electric ship microgrids. *IEEE Transactions on Vehicular Technology*, 68(4):3361–3373, 2019. doi: 10.1109/TVT.2019.2898461.
- [9] Kyaw Hein, Yan Xu, Gary Wilson, and Amit K Gupta. Coordinated optimal voyage planning and energy management of all-electric ship with hybrid energy storage system. *IEEE Transactions on Power Systems*, 36(3):2355–2365, 2021. doi: 10.1109/TPWRS.2020.3029331.
- [10] Mohammed Masum Siraj Khan, Md Omar Faruque, and Alvi Newaz. Fuzzy logic based energy storage management system for mvdc power system of all electric ship. *IEEE Transactions on Energy Conversion*, 32(2):798–809, 2017. doi: 10.1109/TEC.2017.2657327.
- [11] Samy Faddel, Ahmed A Saad, Mohamad El Hariri, and Osama A Mohammed. Coordination of hybrid energy storage for ship power systems with pulsed loads. *IEEE Transactions on Industry Applications*, 56(2):1136–1145, 2019.
- [12] Xiuyan Peng and Luo Zhao. Optimization of mvdc power system of all electric ship based on hybrid energy storage. In *2019 IEEE International Conference on Mechatronics and Automation (ICMA)*, pages 1004–1009. IEEE, 2019.
- [13] Jun Hou, Ziyu Song, Hyeongjun Park, Heath Hofmann, and Jing Sun. Implementation and evaluation of real-time model predictive control for load fluctuations mitigation in all-electric ship propulsion systems. *Applied Energy*, 230:62–77, 2018. ISSN 0306-2619.
- [14] Ali Haseltalab and Rudy R Negenborn. Model predictive maneuvering control and energy management for all-electric autonomous ships. *Applied Energy*, 251:113308, 2019. ISSN 0306-2619.
- [15] Javad Khazaei. Optimal flow of mvdc shipboard microgrids with hybrid storage enhanced with capacitive and resistive droop controllers.

- IEEE Transactions on Power Systems*, 36(4):3728–3739, 2021. doi: 10.1109/TPWRS.2021.3049343.
- [16] Naireeta Deb, Gokhan Ozkan, Phuong H. Hoang, Behnaz Papari, Payam Ramezani Badr, and Christopher Shannon Edrington. An intelligent load shedding scheme for the micro-grid in shipboard power system using probabilistic methods. In *2020 Clemson University Power Systems Conference (PSC)*, pages 1–6, 2020. doi: 10.1109/PSC50246.2020.9131191.
- [17] JA Momoh, JZ Zhu, and SS Kaddah. Optimal load shedding study of naval-ship power system using the everett optimization technique. *Electric Power Systems Research*, 60(3):145–152, 2002.
- [18] Gregory L. Sinsley, Daniel F. Opila, Eun S. Oh, and John D. Stevens. Upper bound performance of shipboard power and energy systems for early-stage design. *IEEE Access*, 8:178600–178613, 2020. doi: 10.1109/ACCESS.2020.3027519.
- [19] Hyeonjun Park, Jing Sun, Steven Pekarek, Philip Stone, Daniel Opila, Richard Meyer, Ilya Kolmanovsky, and Raymond DeCarlo. Real-time model predictive control for shipboard power management using the ipa-sqp approach. *IEEE Transactions on Control Systems Technology*, 23(6):2129–2143, 2015. doi: 10.1109/TCST.2015.2402233.
- [20] Zhiping Ding, Sanjeev K Srivastava, David A Cartes, and Siddharth Suryanarayanan. Dynamic simulation-based analysis of a new load shedding scheme for a notional destroyer-class shipboard power system. *IEEE Transactions on Industry Applications*, 45(3):1166–1174, 2009.
- [21] Arun Shrestha, Edward L. Foulks, and Robert W. Cox. Dynamic load shedding for shipboard power systems using the non-intrusive load monitor. In *2009 IEEE Electric Ship Technologies Symposium*, pages 412–419, 2009. doi: 10.1109/ESTS.2009.4906545.
- [22] Qimin Xu, Bo Yang, Qiaoni Han, Yazhou Yuan, Cailian Chen, and Xinping Guan. Optimal power management for failure mode of mvdc microgrids in all-electric ships. *IEEE Transactions on Power Systems*, 34(2):1054–1067, 2018.
- [23] Jia Li, Feng Liu, Ying Chen, Chengcheng Shao, Guanqun Wang, Yunhe Hou, and Shengwei Mei. Resilience control of dc shipboard power systems. *IEEE Transactions on Power Systems*, 33(6):6675–6685, 2018.
- [24] Kexing Lai and Mahesh S Illindala. Graph theory based shipboard power system expansion strategy for enhanced resilience. *IEEE Transactions on Industry Applications*, 54(6):5691–5699, 2018.
- [25] Kexing Lai and Mahesh S Illindala. A distributed energy management strategy for resilient shipboard power system. *Applied Energy*, 228: 821–832, 2018.
- [26] Chris S Edrington, Gokhan Ozkan, Behnaz Papari, David E Gonsoulin, Dallas Perkins, Tuyen V Vu, and Hesam Vahedi. Distributed energy management for ship power systems with distributed energy storage. *Journal of Marine Engineering & Technology*, 19(sup1):31–44, 2020.
- [27] Mohamed A Mohamed, Hossein Chabok, Emad Mahrous Awwad, Ahmed M El-Sherbeeney, Mohammed A Elmeligy, and Ziad M Ali. Stochastic and distributed scheduling of shipboard power systems using mfoa-admm. *Energy*, 206:118041, 2020. ISSN 0360-5442.
- [28] Behnaz Papari, Robert Cox, Chris S. Edrington, Gokhan Ozkan, Phuong H. Hoang, and Naireeta Deb. Enhancement of energy management in the shipboard power systems based on recursive distributed load shedding model. In *2019 IEEE Electric Ship Technologies Symposium (ESTS)*, pages 605–611, 2019. doi: 10.1109/ESTS.2019.8847883.
- [29] Xianrong Feng, Karen L. Butler-Purpy, and Takis Zourntos. A multi-agent system framework for real-time electric load management in mvac all-electric ship power systems. *IEEE Transactions on Power Systems*, 30(3):1327–1336, 2015. doi: 10.1109/TPWRS.2014.2340393.
- [30] Xianrong Feng, Karen L. Butler-Purpy, and Takis Zourntos. Multi-agent system-based real-time load management for all-electric ship power systems in dc zone level. *IEEE Transactions on Power Systems*, 27(4):1719–1728, 2012. doi: 10.1109/TPWRS.2012.2194314.
- [31] Samy Faddel, Ahmed A Saad, Tarek Youssef, and Osama Mohammed. Decentralized control algorithm for the hybrid energy storage of shipboard power system. *IEEE Journal of Emerging and Selected Topics in Power Electronics*, 8(1):720–731, 2019.
- [32] Quan Zhou, Mohammad Shahidehpour, Ahmed Alabdulwahab, and Abdullah Abusorrah. A cyber-attack resilient distributed control strategy in islanded microgrids. *IEEE Transactions on Smart Grid*, 11(5):3690–3701, 2020. doi: 10.1109/TSG.2020.2979160.
- [33] Tuyen V. Vu, Bang L.H. Nguyen, Zheyuan Cheng, Mo-Yuen Chow, and Bin Zhang. Cyber-physical microgrids: Toward future resilient communities. *IEEE Industrial Electronics Magazine*, 14(3):4–17, 2020. doi: 10.1109/MIE.2019.2958039.
- [34] Mehrdad Yazdani and Ali Mehrizi-Sani. Distributed control techniques in microgrids. *IEEE Transactions on Smart Grid*, 5(6):2901–2909, 2014. doi: 10.1109/TSG.2014.2337838.
- [35] Aaron M. Cramer, Scott D. Sudhoff, and Edwin L. Zivi. Performance metrics for electric warship integrated engineering plant battle damage response. In *2007 IEEE Electric Ship Technologies Symposium*, pages 22–29, 2007. doi: 10.1109/ESTS.2007.372059.
- [36] ESRDC Team. Model description document notional four zone mvdc shipboard power system model. *ESRDC Website, www.esrdc.com*, 2020.
- [37] ESRDC Team. Model description document notional four zone mvdc shipboard power system model. *ESRDC Website, www.esrdc.com*, 2017.